THE JOURNAL OF BIOLOGICAL CHEMISTRY VOL. 288, NO. 23, pp. 16960–16974, June 7, 2013
Published in the U.S.A.

NHERF2 Protein Mobility Rate Is Determined by a Unique C-terminal Domain That Is Also Necessary for Its Regulation of NHE3 Protein in OK Cells*

Received for publication, March 19, 2013, and in revised form, April 9, 2013 Published, JBC Papers in Press, April 23, 2013, DOI 10.1074/jbc.M113.470799

Jianbo Yang[‡], Varsha Singh[‡], Boyoung Cha[‡], Tian-E Chen[‡], Rafiquel Sarker[‡], Rakhilya Murtazina[‡], Shi Jin[‡], Nicholas C. Zachos[‡], George H. Patterson[§], C. Ming Tse[‡], Olga Kovbasnjuk[‡], Xuhang Li[‡], and Mark Donowitz[‡¶1]

From the [‡]Department of Medicine, Division of Gastroenterology, and [¶]Department of Physiology, The Johns Hopkins University School of Medicine, Baltimore, Maryland 21205 and the [§]Biophotonics Section, National Institute of Biomedical Imaging and Bioengineering, NIH, Bethesda, Maryland 20892

Background: PDZ domain-containing scaffolds, NHERF1-3, anchor NHE3 in the epithelial apical membrane, but their own mobility is unknown.
Results: In renal OK cells, microvillar NHERF1-3 are highly mobile with NHERF2 having the slowest mobility.
Conclusion: NHERF2-restricted mobility is conferred by its C terminus, which is also required for its regulation of NHE3.
Significance: A newly recognized NHERF2 C-terminal domain is functionally important.

Na^+/H^+ exchanger regulatory factor (NHERF) proteins are a family of PSD-95/Discs-large/ZO-1 (PDZ)-scaffolding proteins, three of which (NHERFs 1-3) are localized to the brush border in kidney and intestinal epithelial cells. All NHERF proteins are involved in anchoring membrane proteins that contain PDZ recognition motifs to form multiprotein signaling complexes. In contrast to their predicted immobility, NHERF1, NHERF2, and NHERF3 were all shown by fluorescence recovery after photobleaching/confocal microscopy to be surprisingly mobile in the microvilli of the renal proximal tubule OK cell line. Their diffusion coefficients, although different among the three, were all of the same magnitude as that of the transmembrane proteins, suggesting they are all anchored in the microvilli but to different extents. NHERF3 moves faster than NHERF1, and NHERF2 moves the slowest. Several chimeras and mutants of NHERF1 and NHERF2 were made to determine which part of NHERF2 confers the slower mobility rate. Surprisingly, the slower mobility rate of NHERF2 was determined by a unique C-terminal domain, which includes a nonconserved region along with the ezrin, radixin, moesin (ERM) binding domain. Also, this C-terminal domain of NHERF2 determined its greater detergent insolubility and was necessary for the formation of larger multiprotein NHERF2 complexes. In addition, this NHERF2 domain was functionally significant in NHE3 regulation, being necessary for stimulation by lysophosphatidic acid of activity and increased mobility of NHE3, as well as necessary for inhibition of NHE3 activity by calcium ionophore 4-Br-A23187. Thus, multiple functions of NHERF2 require involvement of an additional domain in this protein.

The microvillus represents that aspect of epithelial cells that provides their unique characteristics. For enterocytes and kidney epithelial cells, the microvillus expands the surface over which absorption and secretion occur (1). NHE3 (SLC9A3) is an Na^+/H^+ exchanger that is primarily localized to the microvilli, is responsible for the majority of small intestinal and renal Na^+ absorption (2, 3), and is highly regulated as part of physiologic function, which includes both stimulation and inhibition (4). Four phylogenetically related PDZ domain-containing scaffolding proteins make up the Na^+/H^+ exchanger regulatory factor (NHERF)[2] family, all of which take part in NHE3 regulation to different degrees, as well as the regulation of multiple other proteins (5, 6). NHERF1 is necessary for protein kinase A-mediated inhibition of NHE3 in rabbit renal brush border membranes (7). NHERF2 is needed for cGMP and carbachol-mediated inhibition (8) as well as LPA and dexamethasone-mediated stimulation of NHE3 (9–11). NHERF3 is necessary for calcium-mediated inhibition (12), although NHERF4 is necessary for calcium stimulation of NHE3 (13). NHERF1, NHERF2, and NHERF3 but not NHERF4 are primarily localized to the brush border (14–16). It has been proposed that PDZ domains of NHERF proteins assemble NHE3, ligand receptors, and other effector molecules into large signaling complexes, which are necessary for NHE3 regulation and localize NHE3 to multiple microvillar pools (4, 17).

Microvilli contain a well organized core structure formed by actin microfilaments that are cross-linked by fimbrin and villin, and are attached to the plasma membrane by other proteins, including myosins, ezrin, and α-actinin-4. Multiple classes of membrane proteins attach to these cytoskeletal structures, and it is assumed that they are relatively immobilized (1, 18). FRAP

* This work was supported in part by National Institutes of Health Grants R01DK26523, R01DK61765, P01DK072084, and K08DK088950 from NIDDK.

[1] To whom correspondence should be addressed: Division of Gastroenterology and Hepatology, Dept. of Medicine, 925 Ross Research Bldg., Johns Hopkins University School of Medicine, 720 Rutland Ave., Baltimore, MD 21205-2195. Tel.: 410-955-9675; Fax: 410-955-9677; E-mail: mdonowit@jhmi.edu.

[2] The abbreviations used are: NHERF, Na^+/H^+ exchanger regulatory factor; EBD, ERM binding domain; LPA, oleoyl-L-α-lysophosphatidic acid sodium salt; NHE, Na^+/H^+ exchanger; FRAP, fluorescence recovery after photobleaching; DS, detergent soluble; DI, detergent insoluble; BCECF-AM, 2′,7′-bis(carboxyethyl)-5,6-carboxyfluorescein-acetoxymethyl ester; ROI, region of interest; PDZ, PSD-95/Discs-large/ZO-1; ERM. ezrin, radixin, moesin.

studies with NHE3 have suggested that there are mobile as well as immobile pools of NHE3 in the microvilli and that under basal conditions NHERF1 and NHERF2 immobilize NHE3 and reduce its mobile fraction (19). In addition, immobilization of NHE3 by NHERF2 through protein-protein interactions is dynamically controlled as part of NHE3 regulation. LPA and D-glucose increase NHE3 activity by stimulated exocytosis (17, 20), whereas calcium ionophore 4-Br-A23187 inhibits NHE3 activity by stimulated endocytosis (21). In both cases, the NHERF2 and NHE3 interaction is disrupted initially and then later restored, correlating with the NHE3 mobility that first increases and then decreases. In interpreting these studies, it was hypothesized that NHERF2 defines a transitional storage pool of NHE3 in the microvillus cleft and that the mobility change of NHE3 reflects its trafficking between the microvillar and intracellular pools going through the transitional storage pool (17, 21).

However, it is still not known how mobile the microvillar NHERF proteins are and how the complexes of NHE3 and NHERF proteins are organized in the microvilli. This study was initiated to examine the mobility of NHERF proteins in the microvillus and to determine whether their mobility was also dynamically regulated as part of the signaling that regulates NHE3 activity. Surprisingly, all NHERF proteins were mostly mobile in the microvilli under basal conditions, and their mobility was not significantly changed by treatment with LPA, forskolin, or 4-Br-A23187, all of which alter NHE3 activity. However, there were differences between the NHERFs in their diffusion coefficients, with NHERF2 being more fixed than NHERF1. NHERF1 and NHERF2 are highly homologous structurally to each other but play different roles in the regulation of Na^+ and Cl^- transport (16, 22). The different roles of NHERF1 and NHERF2 in NHE3 regulation have generally been attributed to the different specificities of their PDZ domains via interactions with their PDZ ligands (10, 11, 16). We further focused on defining the NHERF2 region that contributes to its slower mobility rate and determining whether this domain also contributes to its function in NHE3 regulation.

EXPERIMENTAL PROCEDURES

Materials, Plasmids, and Antibodies—Nocodazole and cytochalasin D were from EMD Chemicals (Billerica, MA). Jasplakinolide, BCECF-AM, and nigericin were from Invitrogen. Oleoyl-L-α-lysophosphatidic acid sodium salt (LPA) and OptiPrep were from Sigma. Ca^{2+} ionophore 4-Br-A23187 was from Biomol (Plymouth Meeting, PA). Purified cholera holotoxin was from Sigma and conjugated with Alexa Fluor 790 from Invitrogen. Mouse monoclonal antibodies against FLAG and actin, and anti-FLAG M2 magnetic beads were from Sigma. Mouse monoclonal antibody against NHERF1 was from AbD Serotec (Raleigh, NC). Mouse monoclonal antibody against HA was from Covance, Inc. (Princeton, NJ). Rabbit polyclonal antibody against NHERF2 was a gift from Dr. Chris Yun (23). IRdye-700- or IRdye-800-conjugated goat anti-mouse or goat anti-rabbit secondary antibodies were from Rockland Immunochemicals Inc. (Gilbertsville, PA) and were used with LI-COR Odyssey system (Lincoln, NE) for Western blot analysis. Plasmid pcDNA3.1-HA-NHE3 was constructed previously (24).

Rabbit NHERF1, human NHERF2, and rat NHERF3 were fused to the C terminus of the mCherry tag in the vector pmCherry-C1 (Clontech). NHERF1 was inserted between EcoRI and KpnI to construct pmCherry-NHERF1; NHERF2 was inserted between BglII and SalI to construct pmCherry-NHERF2; NHERF3 was inserted between HindIII and BamHI to construct pmCherry-NHERF3. NHERF1 and NHERF2 were both fused to the FLAG tag in the vector p3×FLAG-CMV-10 (Sigma) between EcoRI and BamHI to construct pFLAG-NHERF1 and pFLAG-NHERF2. To fuse mEOS2 photo-convertible fluorescent protein (25) to the N terminus of NHERFs, a DNA fragment encoding mEOS2 was generated by PCR to replace the sequence coding for mCherry between restriction sites AgeI and BglII in pmCherry-NHERFs vectors to obtain pmEOS2-NHERFs. pmEOS2-NHERF1-PDZ1/2-GAGA and pmEOS2-NHERF2-PDZ1/2-GAGA were generated by QuikChange II site-directed mutagenesis kits (Agilent Technologies, Santa Clara, CA). Four NHERF1 and NHERF2 chimeras were made by PCR with the restriction enzyme site PvuI engineered to connect the fragments (Fig. 6, *A* and *B*). NHERF1-2E and NHERF2-1E were made by switching the ERM binding domains (EBD); NHERF1-2C and NHERF2-1C were made by switching the C terminus, including the nonconserved region and EBD. Another chimera NHERF2-1–2 was made by substituting EBD of NHERF2-1C with that of NHERF2 (Fig. 6*B*).

Cell Culture and Transfection—OK cells were cultured on glass-bottom 35-mm plastic culture dishes (World Precision Instruments Inc.). On the 2nd day post-confluency, OK cells were transfected with 2 μg of plasmid of pmCherry-NHERFs or pmEOS2-NHERFs and other plasmids as indicated, using 10 μl of Lipofectamine 2000 (Invitrogen). The cells were then grown in complete medium overnight and used for FRAP experiments the next day.

The Caco-2/bbe cell line, originally derived from a human adenocarcinoma, was grown on Transwell filter membranes (EMD Millipore) as described previously (8). Caco-2/bbe cells were seeded at $1 \times 10^5/cm^2$ on the filter membranes and grown for 12 days. On the 13th day post-confluency, Caco-2/bbe cells on 6-well Transwell filters were treated with 6 mM EGTA in serum-free Caco-2 medium for 3 h on both the apical and basolateral surfaces. Cells in each well were transfected with 12 μg of pmEOS2-NHERFs using 30 μl of Lipofectamine 2000 on both the apical and basolateral surfaces. Cells were used for FRAP experiments the next day.

FRAP Analysis—FRAP was performed on a stage heated to 37 °C of a Zeiss LSM 510 confocal microscope equipped with a C-Apochromat 63×/1.2 Korr water-immersion objective, as described previously (19). The transfected OK or Caco-2 cells were first washed with DMEM/F-12 media without phenol red twice and incubated in this media for 3 h. Cells were incubated with 30 μM nocodazole for 3 h or 3 μM jasplakinolide for 1 h as indicated. For OK cells, the glass-bottom culture dish could be directly mounted on the microscope stage. For Caco-2 cells, the Transwell filter was cut out, placed on the glass slides with the apical surface outward, covered by a drop of medium, and finally sealed with a coverslip with silicon glue. Cells were kept

on the heated microscope stage for 30 min before beginning the experiment. Optical slices were focused on the cell apical domain with the slice thickness of 3 μm to better tolerate the cell movement in the vertical direction. A square of 3 μm width was used as the region of interest (ROI). Fluorescence within the ROI was measured at low laser power before the bleach and then photobleached with high laser power. Recovery was followed with low laser power at 5- or 10-s intervals usually up to 3–5 min until the intensity had reached a steady plateau. For mEOS2-tagged NHERFs, argon laser 488 nm was used for fluorescence measurement at 25% power, 1% transmission, and for bleaching at 25% power, 100% transmission to about 20–40% of initial fluorescence. To measure fluorescence of mCherry-tagged NHERFs, a HeNe 561-nm laser was used at 4% transmission. To quench fluorescence of mCherry-tagged NHERFs, argon lasers 477, 488, and 514 nm were used at 80% power, 100% transmission in combination with 100% transmission of the HeNe 561-nm laser. mCherry was relatively resistant to quenching with maximal quench about 50%. Fluorescence of an ROI was also measured without bleaching with a high power laser and was used to correct for the bleaching effect caused during measurement. The recovery ratios are calculated as the percentage of maximal bleached fluorescence. More than 12 cells from each experimental group were quantified, and the data presented are representative of three experiments. To calculate the effective one-dimensional diffusion constant (D_{eff}), the experimental data were fit to the Ellenberg equation (26) as reported previously (19). Mobility changes of NHE3-EGFP by LPA/LPA5 (LPA_5 receptor) in the presence of wild type NHERF2 and NHERF2-1C chimera were studied by FRAP as described previously (17).

Photoconversion Experiment—mEOS2 fluorescence conversion was performed in live cells with C-Apochromat 63×/1.2 Korr water-immersion objective on a Zeiss LSM 510 confocal microscope similar to that reported previously (27). Photoconversion of mEOS2-NHERFs was achieved using 100 iterations of 4% 30-milliwatt 405-nm diode laser at the back aperture of the lens with setting at zoom 3.0 and 2.56 μs/pixel. Photoconversion takes ~10–20 s depending on the size of ROI. The green (nonactivated) fluorescence of mEOS was imaged with the argon 488-nm laser, and emission was collected over a range of 505–550 nm. The red (activated) fluorescence of mEOS was imaged with the HeNe 561-nm laser, and emission was collected with a 575–615-nm bandpass emission filter. Pinhole size was adjusted to set the optical slice thickness at 3 μm.

OptiPrep or Sucrose Gradient Ultracentrifugation for Lipid Raft Flotation—Methods were slightly modified from that previously reported (28). OK cells were transiently transfected with pFLAG-NHERFs at 90% confluency and used 2 days after transfection. The cells were homogenized by passing them through a 1-ml syringe/26-gauge needle in TNE buffer A containing 25 mM Tris, pH 7.4, 150 mM NaCl, 50 mM NaF, 5 mM EDTA, 1 mM Na_3VO_4, and protease inhibitors. Nuclei and debris were removed by centrifugation at 3000 × *g* for 15 min at 4 °C. The total membranes were pelleted by ultracentrifugation at 100,000 × *g* for 30 min at 4 °C. Total membranes were then solubilized with cold buffer A supplemented with 0.5% Triton X-100 and then incubated at 4 °C for 30 min on a rotary shaker. Samples were adjusted to 45% of OptiPrep (final volume, 1 ml) before being overlaid with step gradients, 2 ml of 40%, 3 ml of 35%, 3 ml of 25%, 2 ml of 15%, and 1 ml of 5% OptiPrep. Each gradient was prepared with TNE buffer A and adjusted to 0.5% Triton X-100. Samples were centrifuged in a Beckman SW41Ti rotor at 40,000 rpm at 4 °C for 4 h. If sucrose gradient was used, solubilized total membranes were adjusted to 45% of sucrose (final volume, 1 ml) before being overlaid with step gradients, 2 ml of 40%, 3 ml of 35%, 3 ml of 20%, and 3 ml of 5% sucrose. Each gradient was prepared with TNE buffer A and adjusted to 0.5% Triton X-100. Samples were centrifuged in a Beckman SW41Ti rotor at 40,000 rpm at 4 °C for 18 h. Twelve fractions were collected from the bottom of the tubes. One-tenth of each fraction was analyzed with SDS-PAGE and Western blotting. GM1 content in each fraction was analyzed by dot-blot with Alexa Fluor 790-conjugated cholera toxin.

Detergent-soluble (DS) and -insoluble (DI) Fractions of Total Membrane—The experiments were performed as described previously (28). Total membranes were prepared as described above, mixed with cold TNE buffer plus 0.5% Triton X-100, incubated at 4 °C for 30 min, and subjected to ultracentrifugation at 100,000 × *g* for 30 min at 4 °C. The supernatant is referred to as the DS fraction. The pellet was resuspended in 1× SDS-PAGE loading buffer (equal volume to the DS fraction) as the DI fraction.

Sucrose Gradient Ultracentrifugation for Complex Size Analysis—Experiments were performed as described previously with slight modification (29). Total membranes were prepared as described above, solubilized with 5% sucrose in TNE buffer plus 0.5% Triton X-100, and incubated at 37 °C for 30 min. 11 ml of step gradients were prepared by overlaying 1 ml each of the following sucrose gradients: 60, 50, 40, 30, 25, 22.5, 20, 17.5, 15, 12.5, and 10%. Each gradient was prepared with the same TNE buffer plus 0.1% Triton X-100. Samples were centrifuged in a Beckman SW41Ti rotor at 40,000 rpm at 4 °C for 16 h. Twenty four fractions were collected. One-fifth of each fraction was analyzed with SDS-PAGE and Western blotting.

Co-immunoprecipitation—OK cells were transiently co-transfected with pcDNA3.1-LPA5R (LPA_5 receptor) or pcDNA3.1-HA-NHE3 and pFLAG-NHERF2 constructs at 90% confluency with empty p3×FLAG-CMV-10 vector as control. Cells were collected 48 h after transfection. Cell lysate was prepared with lysis buffer (25 mM HEPES, pH 7.4, 150 mM NaCl, 50 mM NaF, 1 mM Na_3VO_4, 0.5% Triton X-100, and protease inhibitors). Anti-FLAG M2 magnetic beads were washed with same buffer three times. 0.5 mg of cell lysate were mixed with 5 μl of anti-FLAG M2 magnetic beads and incubated at 4 °C for 3 h on a rotating shaker. Beads were washed with the same lysis buffer four times and eluted with 1.5× Laemmli sample buffer without β-mercaptoethanol. The input and elution samples were analyzed by SDS-PAGE and Western blotting.

Measurement of Na^+/H^+ Exchange Activity—OK cells were seeded on glass coverslips. At about 90% confluency, cells were co-transfected with pcDNA3.1-HA-NHE3 and pFLAG-NHERFs. For LPA study, pcDNA3.1-LPA5R (10) was also co-transfected. Cells were used for activity measurement at 48 h after transfection. Na^+/H^+ exchange activity was determined

with the intracellular pH-sensitive fluorescent dye BCECF-AM as described previously (21, 24) using a Quantamaster fluorometer from Photon Technology International, Inc (Birmingham, NJ). Cells were serum starved overnight before the assay. For LPA treatment, 3 μM LPA was added when the cells were loaded with 10 μM BCECF-AM in Na^+/NH_4Cl medium for 30 min at 37 °C. For ionophore treatment, cells were perfused with tetramethylammonium supplemented with 0.5 μM 4-Br-A23187 for 5 min before perfusion of Na^+ medium. Initial rate at pH 6.2 was calculated as reported previously (24).

Statistical Analyses—Results were presented as means ± S.D. or S.E. as stated. Comparisons were performed by unpaired Student's *t* tests or analysis of variance for multiple comparisons.

RESULTS

mEOS2-tagged NHERFs Are Localized to Apical Microvillus Clusters in OK Cells—mCherry, GFP, or cyan fluorescent protein tags were fused to the N terminus of NHERF1 or NHERF2 for live imaging and were shown not to affect the function of the NHERFs (21, 30–32). In our study, another fluorescent molecule, mEOS2, was fused to the N terminus of NHERF1, NHERF2, and NHERF3. mEOS2 has green fluorescence, which can be switched to red fluorescence by exposure to 405 nm of UV light (25). The localization of mEOS2-NHERFs in OK cells was studied by transient transfection and live imaging. Two-day post-confluent OK cells were transiently transfected with the plasmids. ~10–20% cells were transfected. Transfected cells showed a large variance in the distribution of mEOS2-NHERFs. mEOS2-NHERF1 and mEOS2-NHERF2 were primarily localized apically in more than 80% of the transfected cells, in which they were present in typical microvillus clusters (Fig. 1*A*), as described previously (33, 34). Each cluster has been shown by electron microscopy to contain several microvilli (33). In the other 20% of cells, mEOS2-NHERF1 and mEOS2-NHERF2 were present abundantly in the cytosol in addition to the microvilli. For mEOS2-NHERF3, only 30% of the transfected cells demonstrated a primarily apical microvillus localization (Fig. 1*A*), although the other cells exhibited a homogeneous cytoplasmic distribution. These results suggest the mEOS2 tag at the N terminus of the NHERFs does not interfere with their microvillus localization. In addition, similar to CFP-NHERF2 (17), mEOS2-NHERF2 is functional in the regulation of NHE3 by calcium ionophore 4-Br-A23187 (data not shown).

NHERFs Are Mostly Mobile but Have Different Diffusion Coefficients—To study the mobility of NHERF proteins in the microvillus, OK cells were transfected with mEOS2-NHERFs as described above, and FRAP experiments were performed. The mEOS2 tags were used to track the NHERF proteins. Only cells with primarily apical localization of NHERFs were used for the study. A small area containing one microvillus cluster was bleached, and the recovery was then monitored. In 5 min, fluorescence of all NHERF proteins recovered almost to the same level as basal (Fig. 1, *B* and *C*). This indicates that all NHERF proteins are mostly mobile, consistent with previous reports in other polarized cell lines (31, 32). For NHERF1 and NHERF2, half of the fluorescence in microvilli was recovered in ~30 and ~80 s, respectively. NHERF3 was even more mobile than NHERF1 with half-recovery time of ~15 s (Fig. 1, *B* and *C*).

Mobility of the NHERFs was also studied with another fluorescent tag, mCherry, to determine whether the mobility was affected by the tags. All NHERFs were fused at the C terminus of mCherry. mCherry-NHERF1 and mCherry-NHERF2 were properly localized to the microvilli, although mCherry-NHERF3 was mostly homogeneously distributed in the cytosol. Similar to the results of mEOS2-tagged NHERFs, FRAP studies showed that mCherry-NHERF1 and mCherry-NHERF2 were highly mobile and that mCherry-NHERF1 recovered faster than mCherry-NHERF2 (Fig. 2*A*).

Data were fit with the Ellenberg equation (26) to calculate mobile fraction and diffusion coefficient. All NHERFs have average mobile fraction close to 100% (Fig. 2*B*). Diffusion coefficients reflect the fluorescence recovery rate, which we will refer to throughout as the mobility rate. Because of experiment to experiment variation in diffusion coefficients, diffusion coefficients were only compared in pairwise experiments done with the same batch of cells on the same day in further studies. In OK cells, mEOS2-NHERF3 has the highest diffusion coefficient, whereas mEOS2-NHERF2 has the lowest among the three NHERFs (Fig. 2*C*). In addition, mEOS2-NHERF1 has a higher diffusion coefficient compared with mEOS2-NHERF2 in Caco-2 cells. It is not known why mCherry-NHERF1 and mCherry-NHERF2 have higher diffusion coefficients than their counterparts with mEOS2 tags and what explains the differences among the cell lines. Nonetheless, NHERF1 consistently has a higher diffusion coefficient compared with NHERF2 (Fig. 2). Because it is easier to transfect OK cells than Caco-2 cells, further studies were performed with OK cells.

Previously, overexpression of NHERF1 and NHERF2 was shown to fix NHE3 to the microvillus, reduce the mobile fraction of NHE3, but not to change the diffusion coefficient (19). However, overexpression of NHE3 did not change the mobility of the NHERFs, including not affecting their diffusion coefficients (data not shown). This was an unexpected result, which we hypothesize is likely due to the presence of multiple additional endogenous brush border proteins with type I PDZ recognition motif, which bind the NHERFs and mask the effect of NHE3 overexpression. In addition, the mobility of NHERFs was not changed by calcium ionophore 4-Br-A23187 and forskolin, which inhibit NHE3 activity, nor by LPA, which stimulates NHE3 activity (data not shown).

Cytoskeleton Does Not Mediate NHERF Mobility—Active transport along microtubules and microfilaments contributes to cellular redistribution of vesicles and proteins. To test whether these processes are involved in the movement of NHERFs, nocodazole was used to interfere with microtubule polymerization, and jasplakinolide was used to prevent actin microfilament disassembly. Neither of these two drugs affected NHERF mobility (Fig. 3). This suggests that NHERF mobility is neither mediated by microtubules nor driven by the treadmilling of actin microfilaments. Cytochalasin D was also used to interfere with actin microfilament assembly. NHERF localization in microvilli was disrupted when OK cells were treated with a high concentration of cytochalasin D for a prolonged time (10 μM, 4 h). When OK cells were treated with a lower

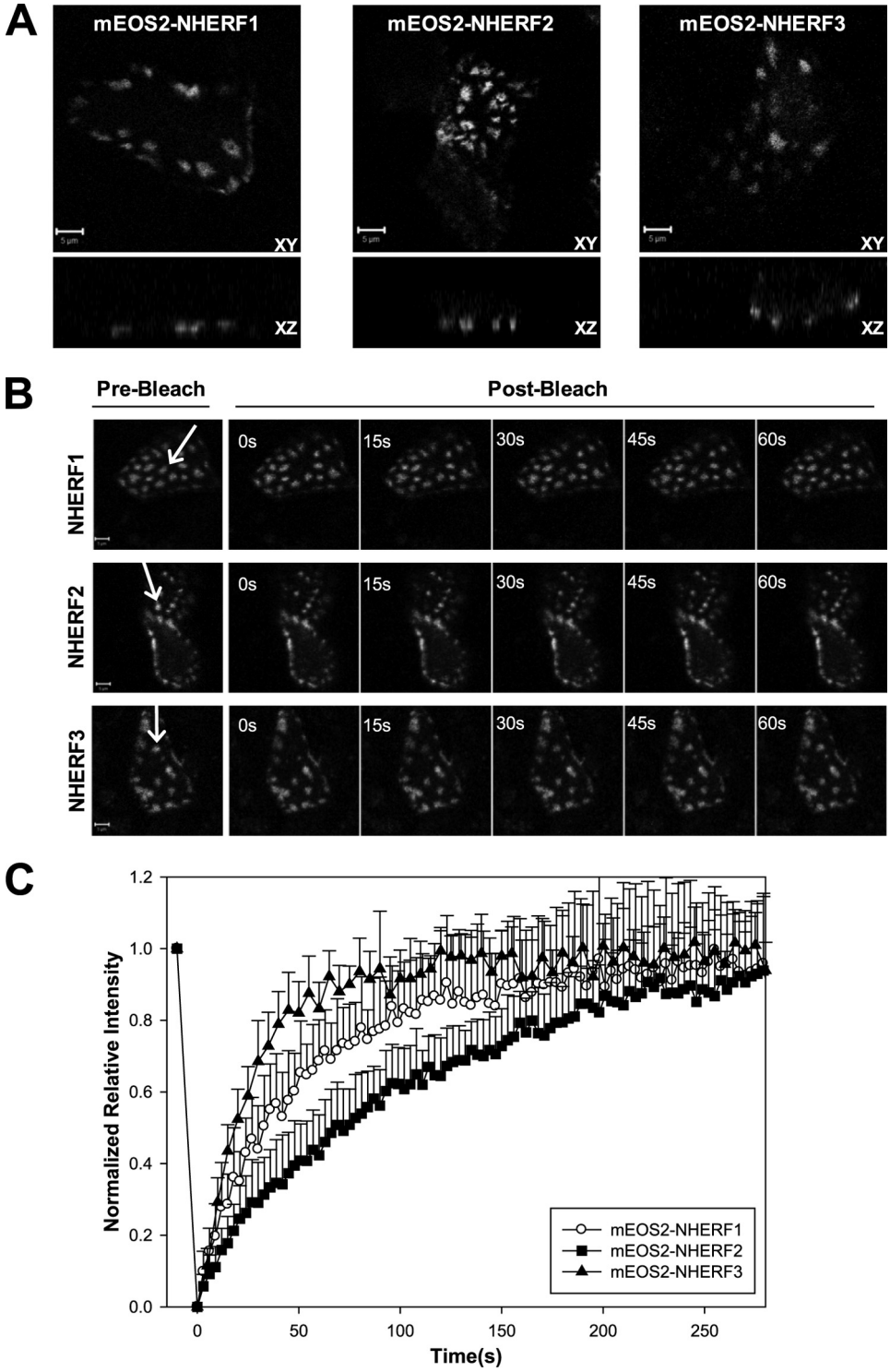

FIGURE 1. **mEOS2-NHERFs are localized to the microvilli in OK cells and are mobile.** *A, top,* XY confocal images of mEOS2-NHERFs were taken at the apical surface of OK cells; *bottom,* XZ images are slices of Z-section. *Bar,* 5 μm. *B,* representative images of FRAP experiments. First images on the *left* are before photo-bleaching. The following images were taken immediately or 15, 30, 45, and 60 s after bleaching. *Arrows* point to the microvillus cluster being bleached. *Bar,* 5 μm. *C,* average recovery curves of mEOS2-NHERF1 (○), mEOS2-NHERF2 (■), and mEOS2-NHERF3 (▲) from 12 cells normalized by total quenched fluorescence intensity. *Error bars* represent S.D.

concentration of cytochalasin D for a short time (5 μM, 20 min), visible microvilli remained, and NHERF mobility was not changed (data not shown). Because it is likely that the actin microfilaments were still intact in these remaining microvilli, it is not possible to interpret the effects of cytochalasin D on the NHERF microvillar mobility.

It is known that a single microvillus cluster contains multiple microvilli (33). FRAP experiments performed by bleaching the intact cluster only gives information about movement of NHERFs among different clusters. If NHERFs exchange faster inside a single cluster than between different clusters, recovery of NHERF fluorescence will be faster when only part of a single

A

cell	Fusion protein	Mobile fraction (%)	Diffusion Coefficient ($x10^{-10}$ cm^2/s)
OK	mEOS2-NHERF1	96 ± 16	6.1 ± 2.6
	mEOS2-NHERF2	106 ± 11	2.4 ± 0.9
	mEOS2-NHERF3	102 ± 20	16.6 ± 5.8
	mCherry-NHERF1	104 ± 18	14.7 ± 4.6
	mCherry-NHERF2	106 ± 19	3.9 ± 1.4
CaCO2	mEOS2-NHERF1	93 ± 7	17.9 ± 4.8
	mEOS2-NHERF2	97 ± 16	2.5 ± 1.1

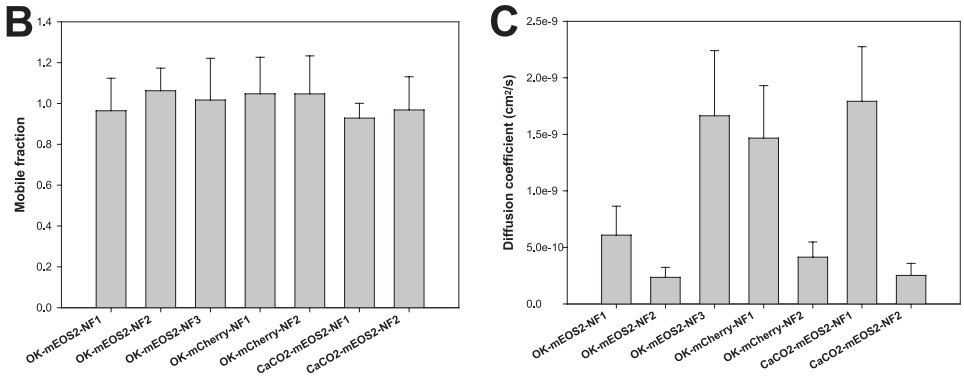

FIGURE 2. **Mobile fractions and diffusion coefficients of NHERFs.** *A,* mobile fractions and diffusion coefficients of NHERFs in OK or Caco-2 cells were derived from experiments and listed in the *table*. Mobile fractions (*B*) and diffusion coefficients (*C*) of mEOS2-NHERFs and mCherry-NHERFs were plotted. Experiments were repeated three times, and in each experiment FRAP data from eight different cells were used for the calculation ($n = 24$, results are mean ± S.D.).

microvillus cluster is bleached. In contrast, fluorescence recovery of all NHERF proteins was not different whether a partial cluster or the intact cluster was bleached (data not shown). This indicates that there is no priority for NHERFs to move to adjacent microvilli within the same cluster.

mEOS2 can be photo-converted from green fluorescence to red fluorescence by exposure to UV light. Using this property, a small area containing a single microvillus cluster was exposed to a 405-nm laser for ~10 s. The mEOS2-NHERF1 in this small region showed red fluorescence immediately after the exposure (Fig. 4). The distribution of this specific pool of red fluorescence-labeled NHERF1 was tracked over time. In less than 2 min, the red fluorescence was equally distributed over the entire apical surface, including the microvillus clusters at the periphery of the cell (Fig. 4). NHERF2 and NHERF3 behaved very similarly. These results indicate that NHERFs are very mobile and move freely among microvillus clusters. However, active transport through the cytoskeleton usually involves spatially restricted movement. The uniform re-distribution of photo-converted mEOS2-NHERFs over the entire apical surface further speaks against the involvement of the cytoskeleton in the movement of the NHERFs.

C Terminus of NHERF2 Is Responsible for Its Slower Mobility—NHERF3 has four PDZ domains and a short C terminus. How NHERF3 is anchored to the microvilli has not been well characterized. NHERF1 and NHERF2 are similar to each other yet play different roles in NHE3 regulation. Further studies focused on comparison between NHERF1 and NHERF2. Both have two conserved PDZ domains (PDZ1 and PDZ2) and a conserved EBD at their C termini. But the sequences between the PDZ1 and PDZ2 domains, and the sequences between PDZ2 and the EBD domain are not conserved. To determine which part of NHERF1 and NHERF2 contributes to their distinct mobilities, several mutants and chimeras were constructed and compared with the wild type.

PDZ domains in NHERF1 and NHERF2 bind to their ligands through a groove formed by the sequence GYGF (35, 36). By substituting the GYGF sequence in both PDZ domains with GAGA, mutants NHERF1-PDZ1/2-GAGA and NHERF2-PDZ1/2-GAGA were made. The binding ability of PDZ domains to most of their ligands are abolished in these mutants (36, 37). Both of the mutants localized to the microvilli similarly to wild type. Fluorescence recovery of mutant NHERF1-PDZ1/2-GAGA was very similar to that of wild type NHERF1 (Fig. 5*A*). Mutant NHERF2-PDZ1/2-GAGA recovered a little faster than wild type NHERF2, but the difference was not statistically significant (Fig. 5*B*). This suggests that ligand binding to PDZ1 or PDZ2 is not the determining factor of the diffusion coefficient of NHERF1 and NHERF2 in OK cells. It also contributes to the result above that overexpression of NHE3 does not change the mobility of NHERF1 and NHERF2.

The NHERF C-terminal EBD has been shown sufficient for ERM binding (38, 39) and necessary for anchoring NHERF1 and NHERF2 to the apical microvilli (21, 40). To test whether the EBD causes the mobility difference between NHERF1 and NHERF2, two chimeras NHERF1-2E and NHERF2-1E were

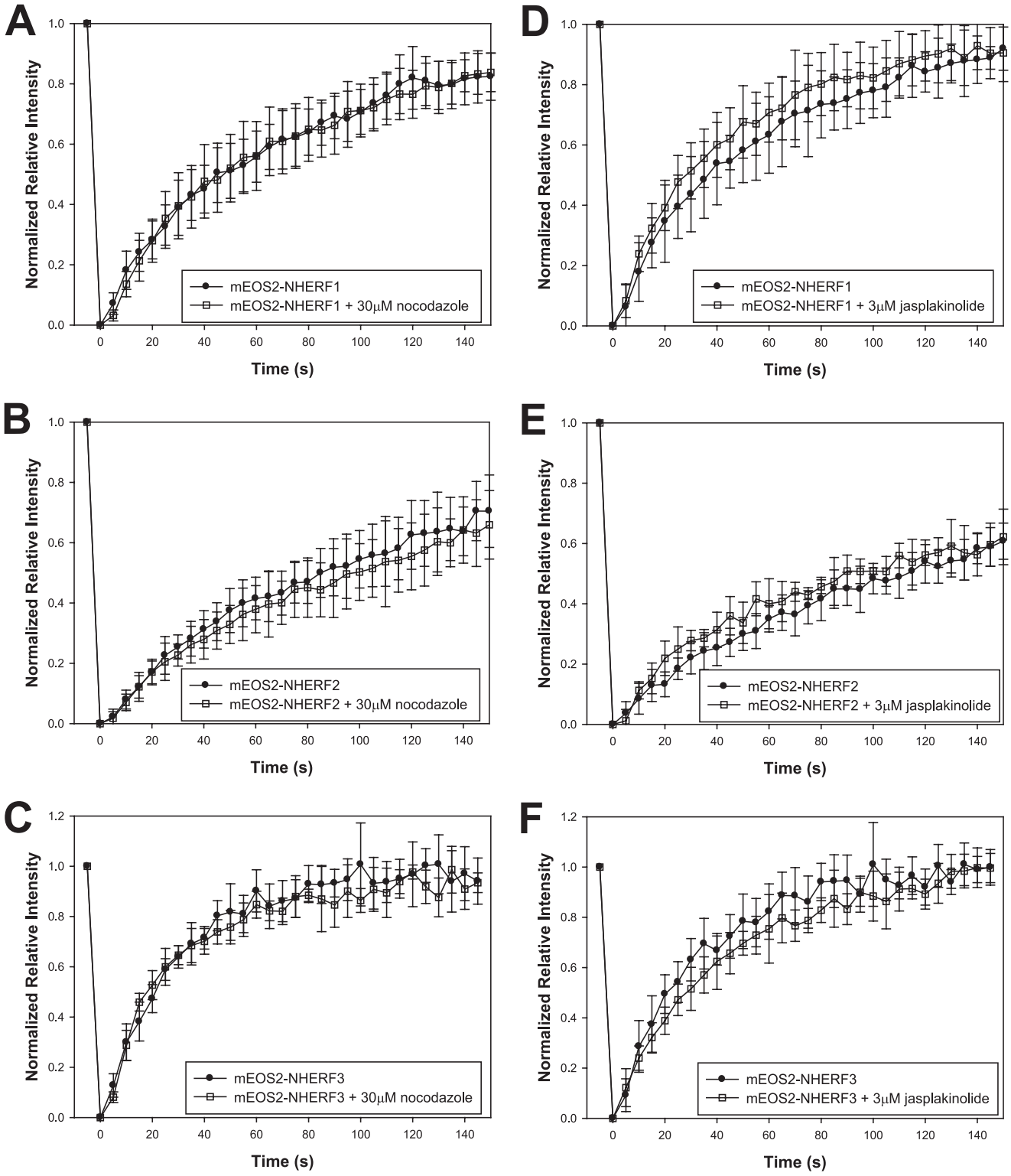

FIGURE 3. **Neither nocodazole nor jasplakinolide significantly affected the mobility of mEOS2-NHERFs in OK cells.** FRAP recovery curves of mEOS2-NHERF1 (*A* and *D*), mEOS2-NHERF2 (*B* and *E*), and mEOS2-NHERF3 (*C* and *F*) in the presence of 30 μM nocodazole (*A–C*) or 3 μM jasplakinolide (*D–F*) were compared with control conditions without treatment. Cells were incubated with 30 μM nocodazole for 3 h or 3 μM jasplakinolide for 1 h before FRAP experiments. Nocodazole or jasplakinolide treatment is represented by □ and control condition is represented by ●. *Error bars* represent S.D. One representative result from three repeated pairwise experiments is shown.

made by switching the EBD between NHERF1 and NHERF2 (Fig. 6, *A* and *B*). We attempted to switch only the EBD domains (C-terminal 30 amino acid residues) of NHERF1 but failed due to technical issues with PCR amplification of the DNA fragments. The sequence switched (marked by *S1* in Fig. 6*A*) contains more than 30 amino acid residues, which include the well defined EBD sequence (38, 39, 41). Chimera NHERF1-2E is the NHERF1 N terminus carrying the EBD of NHERF2. It has the

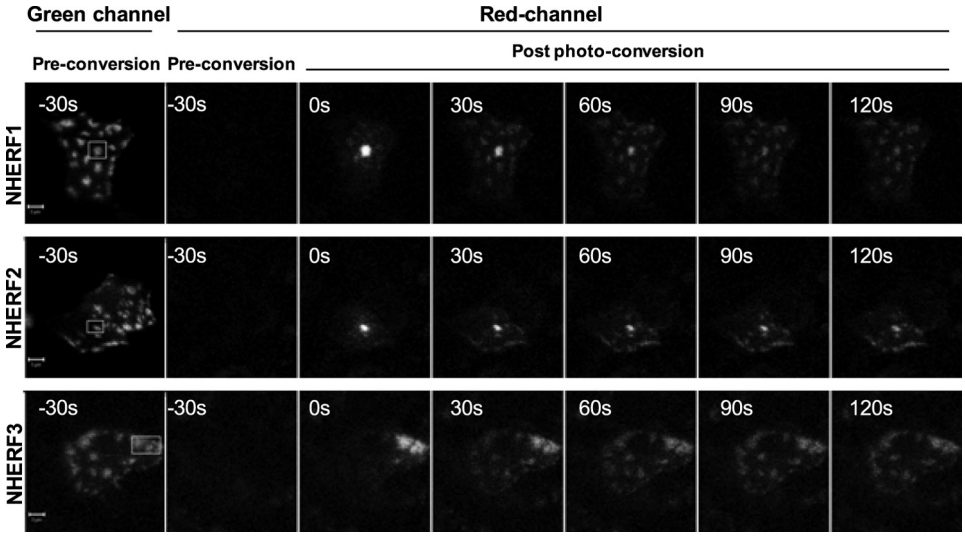

FIGURE 4. **Photo-converted mEOS2-NHERFs redistributed homogeneously over the entire apical microvilli in OK cells.** The first images on the *left* show the green fluorescence of mEOS2-NHERFs on the apical membrane of OK cells before photo-conversion. The second images show there is no red signal before photo-conversion. Then a small area of microvillar clusters, marked by the *box*, was photo-converted from green to red by exposure to UV laser for ~10–20 s. Movement of the red photo-converted mEOS2-NHERFs was monitored every 30 s. *Bar,* 5 μm. Experiments were repeated three times, and representative images are shown.

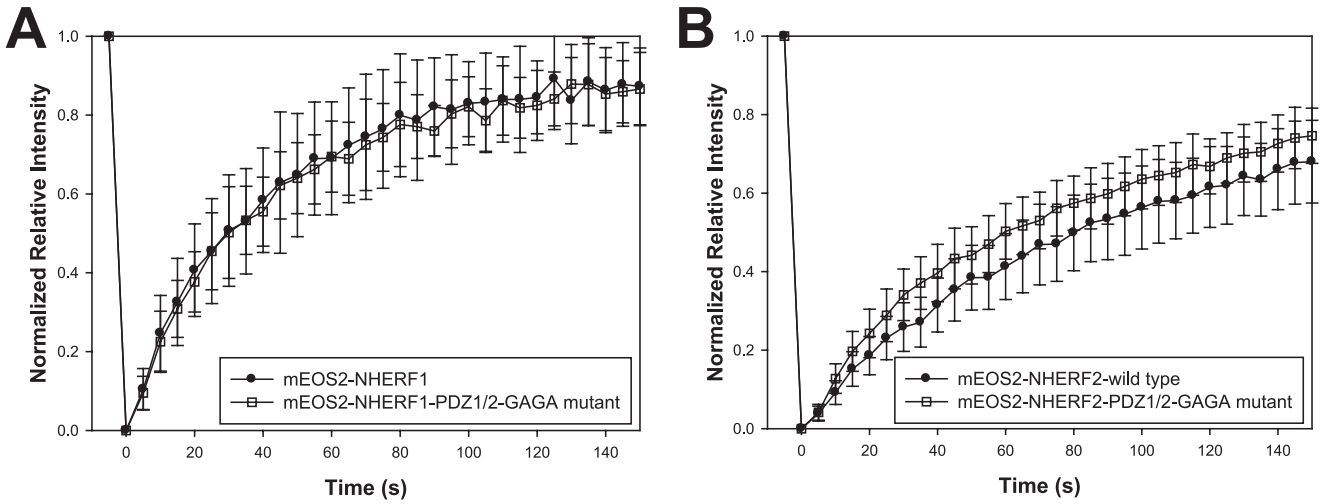

FIGURE 5. **Recovery dynamics of mEOS2-NHERF1 and mEOS2-NHERF2 were independent of PDZ ligand binding.** *A,* fluorescence recovery was compared between wild type mEOS2-NHERF1 (●) and mEOS2-NHERF1-PDZ1/2-GAGA mutant (□), in which PDZ ligand binding groove sequence GYGF were mutated to GAGA in both PDZ domains. *B,* fluorescence recovery was compared between wild type mEOS2-NHERF2 (●) and mEOS2-NHERF2-PDZ1/2-GAGA mutant (□). *Error bars* represent S.D. One representative result from three repeated pairwise experiments is shown.

same mobility rate as wild type NHERF1 (Fig. 6*C*). However, the NHERF2-1E chimera carrying the EBD of NHERF1 has a faster recovery rate than wild type NHERF2, which approaches wild type NHERF1 (Fig. 6*C*). This suggests that the EBD of NHERF2 is required for the slower mobility rate of NHERF2 but does not sufficiently confer this phenotype to NHERF1.

Because the sequences between PDZ2 and EBD are not conserved between NHERF1 and NHERF2 (Fig. 6*A*), we hypothesized that this unique region plus the EBD of NHERF2 together might determine the slower mobility rate of NHERF2. To test this hypothesis, two additional chimeras were made by switching the C terminus (marked by *S2* in Fig. 6*A*), which includes the unique region plus the EBD. Chimera NHERF2-1C is the NHERF2 N terminus plus the C terminus of NHERF1. It has a faster recovery rate than wild type NHERF2 (Fig. 6*D*). Chimera NHERF1-2C, which has the C terminus of NHERF2, has a slower recovery rate than wild type NHERF1, almost as slow as wild type NHERF2 (Fig. 6*D*). This indicates that the C terminus of NHERF2, which includes both the EBD and the nonconserved sequences between PDZ2 and EBD, determines the slower mobility rate of NHERF2. Because a small portion of the nonconserved region of NHERF1 was also switched when the chimeras NHERF1-2E and NHERF2-1E were made, it is not known whether the nonconserved region of NHERF1 also functions collaboratively with its EBD.

Slower NHERF Mobility Rates Correlate with Greater Detergent Insolubility and Larger Complex Size—NHERF1 has been suggested to anchor lipid rafts in the plasma membrane to the cytoskeleton and help set the mobility of lipid rafts (42). This caused us to test whether lipid raft association affects the NHERF mobility rate. In studies done in HEK293 cells using sucrose gradient ultracentrifugation and flotillin-1 as a lipid raft

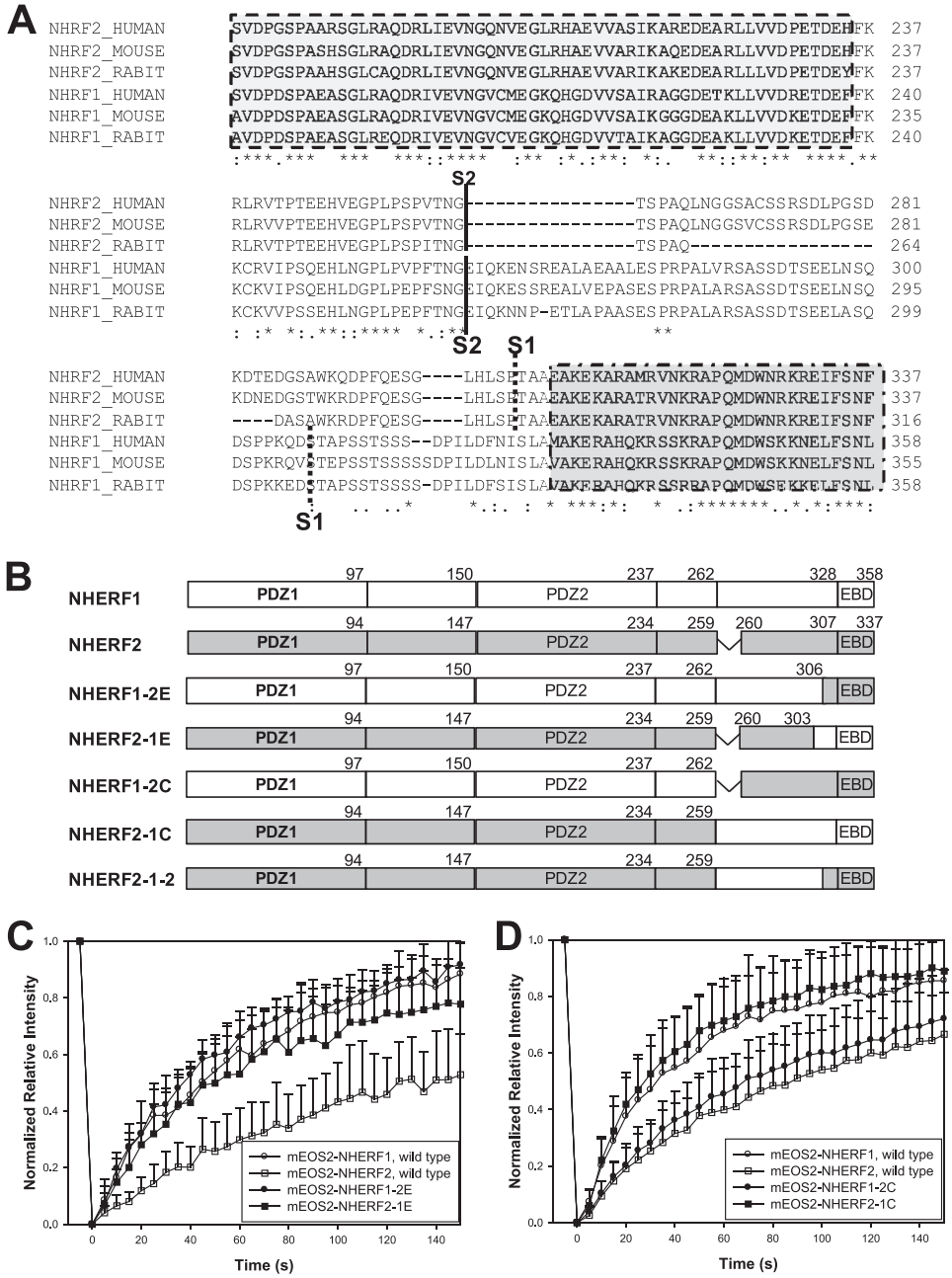

FIGURE 6. **Recovery dynamics of mEOS2-NHERF1 and mEOS2-NHERF2 were determined by their C termini.** *A,* sequence alignment of C-terminal part of NHERF1 and NHERF2. Sequences of NHERF1 and NHERF2 from *Homo sapiens*, *Mus musculus,* and *Oryctolagus cuniculus* were aligned with ClustalW software. Part of PDZ2 domain is framed by *dash lines*. EBD is framed by *dash-dot lines*. Lines labeled with *S1* are the positions switched to make NHERF1-2E and NHERF2-1E chimeras. Lines labeled with *S2* are the positions switched to make NHERF1-2C and NHERF2-1C chimeras. *B,* domain architectures of wild type NHERF1, NHERF2, and five chimeras. *White rectangles* represent sequences from NHERF1, and *gray rectangles* represent sequences from NHERF2. *Numbers* on the top of the *rectangles* represent the numbers of the amino acid residues. *C,* fluorescence recovery was compared among wild type mEOS2-NHERF1 (○), mEOS2-NHERF2 (□), chimera mEOS2-NHERF1-2E (●), and mEOS2-NHERF2-1E (■). The data points of mEOS2-NHERF2 after 20 s are significantly different from that of other constructs ($p < 0.05$). *D,* fluorescence recovery was compared among wild type mEOS2-NHERF1 (○), mEOS2-NHERF2 (□), chimera mEOS2-NHERF1-2C (●), and mEOS2-NHERF2-1C (■). The data points of mEOS2-NHERF1 after 15 s are significantly different from that of mEOS2-NHERF1-2C ($p < 0.05$), and the data points of mEOS2-NHERF2 after 15 s are significantly different from that of mEOS2-NHERF2-1C ($p < 0.05$). *Error bars* represent S.D. One representative result from three repeated pairwise experiments is shown.

marker, NHERF2 associated with lipid rafts more strongly than NHERF1 (43). Of note, in another study with rabbit ileum using OptiPrep gradient ultracentrifugation, neither NHERF1 nor NHERF2 were associated with lipid rafts based on the criterion that lipid rafts can be shifted to heavier fractions by methyl-β-cyclodextrin (28). To analyze the lipid raft association of NHERF1 and NHERF2 in OK cells, total membranes were prepared and subjected to lipid raft flotation analysis with GM1 gangliosides as the marker of lipid rafts. Both sucrose gradients and OptiPrep gradients gave the same conclusions that NHERF1 and NHERF2 were poorly associated with lipid rafts in this model with no significant difference (Fig. 7). NHERF1 has 4.9 ± 1.8% (mean ± S.E., $n = 3$) in lipid raft fractions, whereas NHERF2 has 5.0 ± 1.3% (mean ± S.E., $n = 3$) in lipid raft

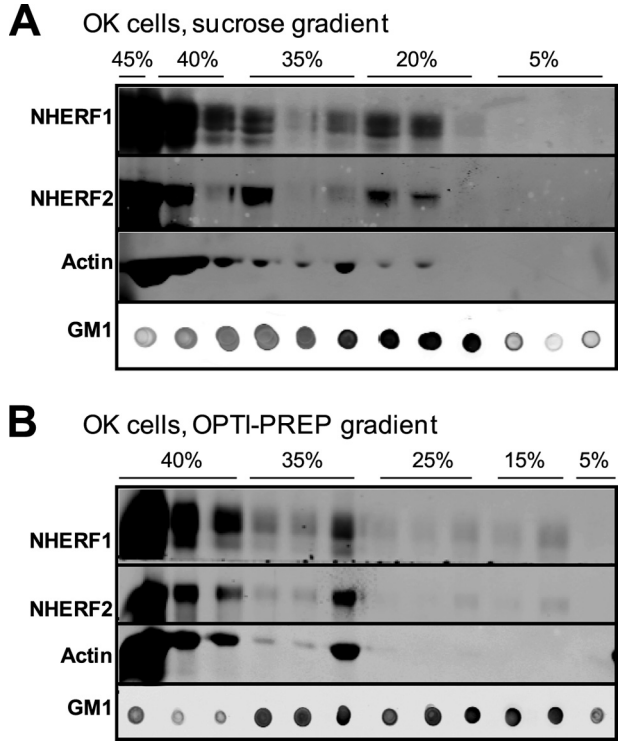

FIGURE 7. **NHERF1 and NHERF2 do not show significant differences in lipid raft association.** OK cells were transiently transfected with pFLAG-NHERF1 and pmEOS2-NHERF2. Total membranes were subjected to lipid raft flotation analysis by sucrose gradient (*A*) or OptiPrep gradient (*B*) as described under "Experimental Procedures." NHERF1 was probed with mouse monoclonal anti-FLAG. NHERF2 was probed with rabbit polyclonal anti-NHERF2. GM1 was analyzed by dot-blotting with Alexa Fluor 790-conjugated cholera toxin. Experiments were repeated three times, and one representative result is shown.

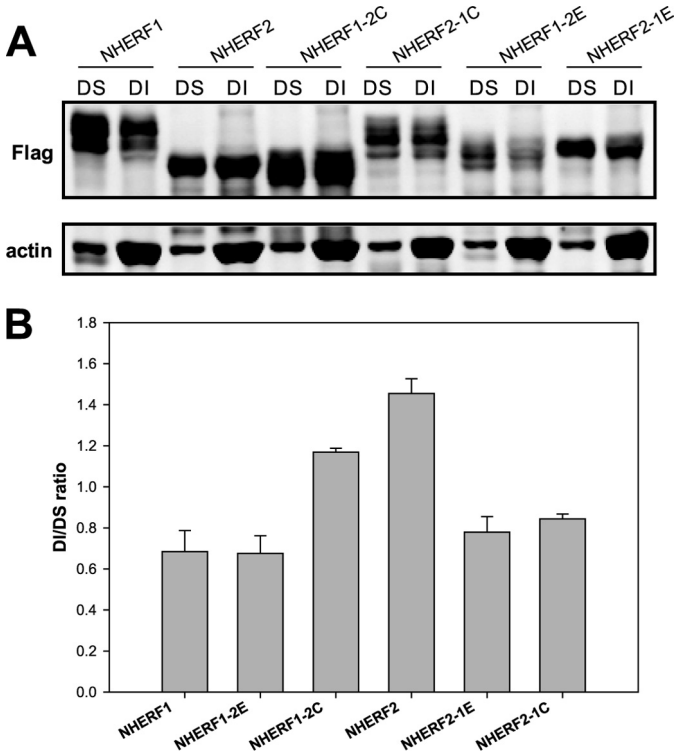

FIGURE 8. **C terminus of NHERF2 also determines the DS and DI distribution.** *A,* total membranes were prepared from OK cells transiently transfected with pFLAG-NHERF1 or NHERF2 constructs and then separated into DS and DI fractions by treating with 0.5% Triton X-100 buffer at 4 °C. All NHERFs were probed with mouse monoclonal anti-FLAG. *B,* experiments were repeated three times. The intensity of the band was quantitated by densitometry, and the DI/DS ratio was derived from the intensities. *Error bars* represent S.E.

fractions. This suggests that lipid raft association is unlikely to account for the differences of mobility rates between NHERF1 and NHERF2.

In contrast, NHERF1 and NHERF2 had different distributions, when total membranes were separated into DS and DI fractions by treating total membranes with cold 0.5% Triton X-100 buffer at 4 °C and centrifuging at 100,000 × *g*. ~40% of NHERF1 was in the DI and ~60% in the DS fraction (Fig. 8), and ~60% of NHERF2 was in the DI and ~40% in the DS fraction. After switching the C termini between NHERF1 and NHERF2, chimera NHERF1-2C had an increased presence in the DI fraction. Oppositely, NHERF2-1C chimera had a reduced presence in the DI fraction compared with NHERF2. If only the EBDs were switched, both the NHERF1-2E and NHERF2-1E chimeras were less in the DI than the DS. For both wild type and the NHERF chimeras, a higher percentage distribution in the DI fraction correlated with a slower mobility rate (Figs. 6 and 8).

The DI fraction contains lipid rafts and cytoskeleton complexes (28, 44). Because NHERF1 and NHERF2 do not have significant differences in lipid raft association, it was hypothesized that they might associate with cytoskeletal elements differently. Total membranes were treated with 0.5% Triton X-100 at 37 °C to dissolve lipid rafts. The solubilized membranes were subjected to size fractionation with sucrose gradient ultracentrifugation. Initially, mEOS2-NHERF2 and FLAG-NHERF1 were co-transfected in the same cell for comparison of their relative distributions. Although there was some overlap in the fractions in which mEOS2-NHERF2 and FLAG-NHERF1 were distributed, NHERF2 had a greater distribution than NHERF1 in the heavier fractions (Fig. 9*A*). Given the relatively large size of the mEOS2 tag (about 230 amino acid residues), further studies were performed with endogenous NHERF1 and FLAG-tagged NHERF1/NHERF2 constructs. FLAG-NHERF2 appears in heavier fractions compared with endogenous NHERF1 in OK cells (Fig. 9*B*), indicating that this distribution is a feature of NHERF2 compared with NHERF1 and is not caused by the relatively large size of the mEOS2 tag. This suggests that NHERF2 interacts with its partners strongly enough to form stable larger complexes. To test whether this is contributed to by the C terminus of NHERF2, NHERF1 was compared with chimera NHERF1-2C (Fig. 9*C*), and NHERF2 was compared with chimera NHERF2-1C (Fig. 9*D*). Chimera NHERF1-2C (NHERF2 C terminus) was in the heavier fractions, and chimera NHERF2-1C (NHERF1 C terminus) was in the lighter fractions. These results suggest that the C terminus of NHERF2 is required to form stable large complexes, either by binding different partners than NHERF1 or via stronger interactions with some of the same partners that bind to NHERF1.

Nonconserved Domain in the C Terminus of NHERF2 Is Necessary for NHE3 Regulation—NHERF proteins play important roles in NHE3 regulation (16, 22). NHERF2 but not NHERF1 is required for stimulation of NHE3 by LPA (10, 45) and inhibition of NHE3 by carbachol and calcium ionophore 4-Br-

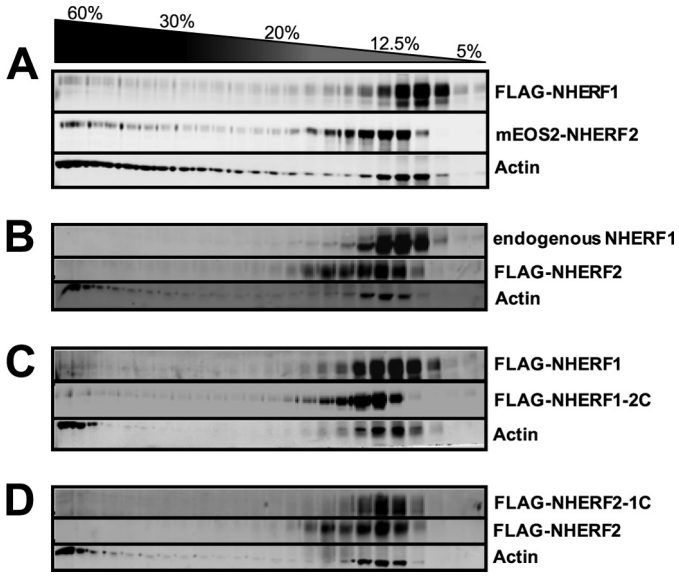

FIGURE 9. **NHERF proteins carrying the C terminus of NHERF2 were associated with membrane in larger complexes determined by sucrose gradient ultracentrifugation.** Total membranes were prepared from OK cells transiently transfected with pmEOS2-NHERF2 and pFLAG-NHERF1 (*A*), pFLAG-NHERF2 (*B*), pFLAG-NHERF1 and pFLAG-NHERF1-2C (*C*), and pFLAG-NHERF2-1C and pFLAG-NHERF2 (*D*) and then were subjected to complex size analysis as described under "Experimental Procedures." *A,* FLAG-NHERF1 was probed with mouse monoclonal anti-FLAG, and mEOS2-NHERF2 was probed with rabbit polyclonal anti-NHERF2. *B,* NHERF1 was probed with mouse monoclonal anti-NHERF1, and FLAG-NHERF2 was probed with rabbit polyclonal anti-NHERF2 antibodies. *C,* FLAG-NHERF1 was probed with mouse monoclonal anti-FLAG, and FLAG-NHERF1-2C was probed with rabbit polyclonal anti-NHERF2 (recognizing NHERF2 C terminus). *D,* FLAG-NHERF2-1C was probed with mouse monoclonal anti-FLAG antibodies, and FLAG-NHERF2 was probed with rabbit polyclonal anti-NHERF2. Experiments were repeated three times, and one representative result is shown.

A23187 (21, 46). Although emphasis has been on the role of the NHERF PDZ domains in the regulatory function of this gene family, we determined whether the C terminus of NHERF2 is also important for regulation of NHE3 activity. By co-immunoprecipitation, NHERF2 chimeras bound to NHE3 at the same level as wild type NHERF2 (Fig. 10*A*). When NHERF2 was overexpressed in OK cells, calcium ionophore 4-Br-A23187 significantly reduced NHE3 activity (Fig. 10*B*) as reported previously (21). However, chimera NHERF2-1C and NHERF2-1E were not able to support this inhibition (Fig. 10*B*). In Caco-2 cells, LPA_5 receptor and NHERF2 are involved in LPA-dependent NHE3 stimulation (10). Overexpression of NHERF2 and LPA_5 receptor also confers LPA-dependent NHE3 stimulation in OK cells[3] as shown in Fig. 10*C*. LPA was not able to stimulate NHE3 activity when the NHERF2-1C or NHERF2-1E was co-expressed with LPA_5 receptor in OK cells (Fig. 10*C*), although chimeras still interacted with LPA_5 receptor normally (Fig. 10*A*). To further test whether the loss of NHERF2 function in NHE3 regulation is solely due to substitution of the EBD of NHERF2, another chimera NHERF2-1–2 was made in which only the nonconserved sequence between PDZ2 and EBD, but not the EBD, was substituted (Fig. 6). Chimera NHERF2-1–2 was not able to support either stimulation of NHE3 by LPA or inhibition of NHE3 by calcium ionophore 4-Br-A23187 (Fig. 10). These results suggest that the NHERF2 nonconserved

[3] T. Chen, B. Cha, and M. Donowitz, unpublished data.

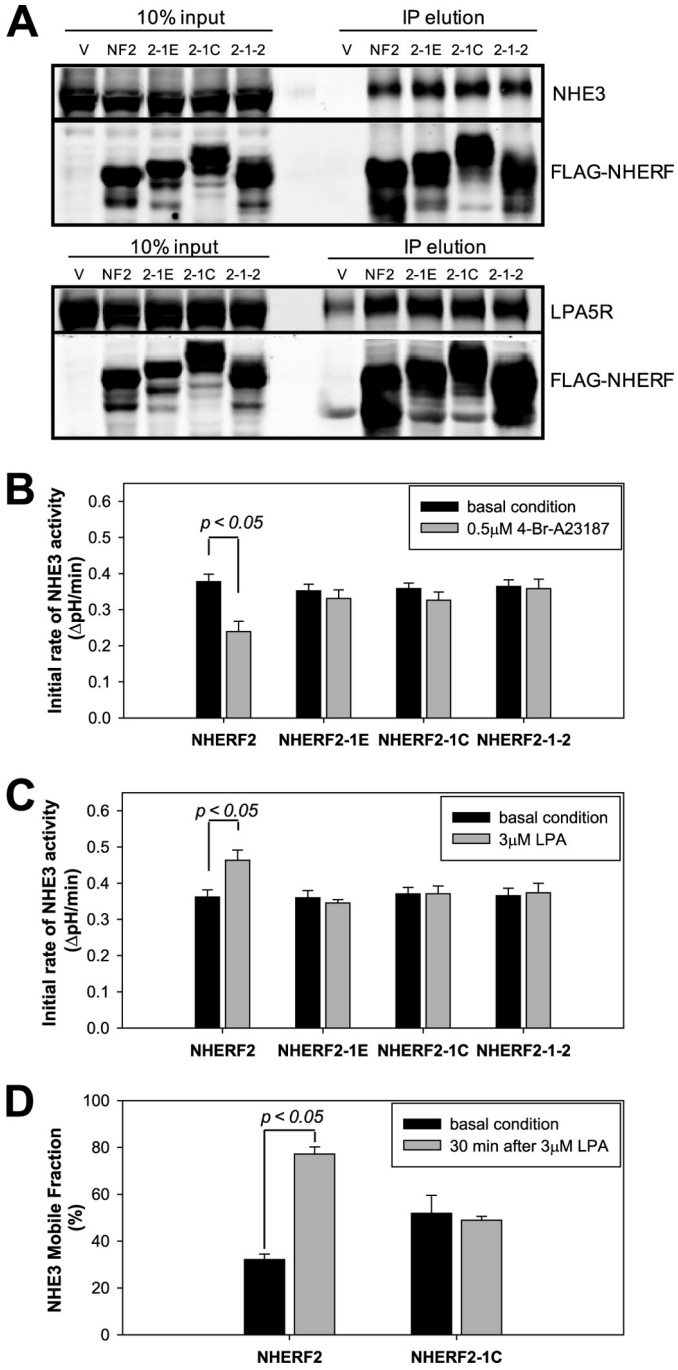

FIGURE 10. **NHERF2 loses the ability to support NHE3 inhibition by calcium ionophore 4-Br-A23187 and stimulation by LPA when its C terminus is substituted with the C terminus of NHERF1.** *A,* NHE3 and LPA5R were co-immunoprecipitated (*IP*) with FLAG-NHERF2 constructs (pFLAG-NHERF2, pFLAG-NHERF2-1E, pFLAG-NHERF2-1C, or pFLAG-NHERF2-1–2) as described under "Experimental Procedures." LPA5R and NHE3 are both fused with the HA tag and probed with mouse monoclonal anti-HA. FLAG-NHERF2 was probed with mouse monoclonal anti-FLAG. Empty p3×FLAG-CMV-10 vector (*V*) was used as control. *B,* OK cells were transiently co-transfected with pcDNA3.1-HA-NHE3 and NHERF2 constructs as indicated. NHE3 activity was measured in the absence (*black bar*) and presence (*gray bar*) of 0.5 μM 4-Br-A23187 ($n = 5$). *C,* OK cells were transiently co-transfected with pcDNA3.1-HA-NHE3, pcDNA3.1-LPA5R, and FLAG-NHERF2 constructs as indicated. NHE3 activity was measured in the absence (*black bar*) and presence (*gray bar*) of 3 μM LPA ($n = 5$). *D,* OK cells were transiently co-transfected with pcDNA3.1-NHE3-GFP, pcDNA3.1-LPA5R, and FLAG-NHERF2 constructs as indicated. NHE3 mobility was measured at basal condition (*black bar*) and 30 min after the treatment with 3 μM LPA (*gray bar*) ($n = 3$). *Error bars* represent S.E.; results with no *p* value labeled are not significantly different.

sequence after PDZ2, either alone or with the EBD, is required for NHE3 regulation.

NHERF2 overexpression decreased NHE3 mobility in the apical domain of Caco-2 and OK cells (19, 20). Also, the mobility of NHE3 was transiently increased upon NHERF2-dependent stimulation by LPA, which was accompanied by dissociation of NHE3 from NHERF2 (17). The effect of chimera NHERF2-1C on NHE3 mobility was determined in OK cells (Fig. 10*D*). NHE3 has basal mobile fraction (M_f) ~30% when wild type NHERF2 was overexpressed, consistent with previous results (19). Basal M_f of NHE3 was ~50% when NHERF2-1C was overexpressed. This indicates that NHERF2-1C limits NHE3 mobility less than does wild type NHERF2, consistent with its relative faster mobility rate compared with that of wild type NHERF2. In the presence of wild type NHERF2, NHE3 M_f increased to ~70% at 30 min after LPA treatment. In contrast, NHE3 mobility did not change after LPA treatment when the chimera NHERF2-1C was studied. This shows that the NHERF2 C terminus is required for both setting the basal M_f of NHE3 and the increase of NHE3 mobility triggered by LPA.

DISCUSSION

Although the epithelial cell microvillus is thought of as a stable structure related to the presence of a large cytoskeletal component, this view is almost certainly incorrect. In fact, microvillar actin, ezrin, and MYO1A (myosin I) rapidly turn over, as shown by FRAP studies (47–49). In this study, microvillar NHERF1, NHERF2, and NHERF3 similarly turned over rapidly. Photo-converted mEOS2-NHERFs moved freely over the entire apical surface with no preference to any direction. This is opposite to the spatially limited and directed movement predicted for cytoskeleton-mediated transport. Therefore, the mobility of apical NHERFs most likely reflects the dynamic exchange between cytoskeleton or membrane-associated pools and nonassociated pool in the microvillus. A similar model has been described in which it was suggested that ezrin exchanges among three pools, the free cytosolic pool, less mobile membrane-associated pool, and immobile actin-bound pool (47).

The three NHERFs had diffusion coefficients in the range of $1–10 \times 10^{-10}$ cm^2/s. This is similar to that of transmembrane proteins such as NHE3 and cystic fibrosis transmembrane regulator (19, 30). In contrast, a free cytosolic protein such as GFP has a diffusion coefficient in the range of 1×10^{-7} cm^2/s (30). This is consistent with all NHERF proteins being anchored to the cytoskeleton and/or the membrane, although not totally fixed. ~30% of NHE3 is immobile in OK cells under basal conditions (19), although NHERF proteins do not have a significant immobile fraction. This means that NHE3 is not solely immobilized by NHERF proteins. But NHERF proteins likely synergize with other immobilizing mechanisms to contribute to the fixation of brush border proteins such as NHE3, PMCA2w/b (34), and Npt2a (50). For instance, because NHERF1/2 interacts with ezrin, which also directly binds to NHE3, the synergistic effect on NHE3 anchoring would be expected between NHERF1/2 and ezrin (51). In addition, NHE3 has also been shown to bind Shank2, which also functions as a scaffold (52). We thus suggest that this reported immobilization of NHE3 by NHERF proteins represents a state of dynamic equilibrium rather than a static immobile state (19). This is likely to confer an advantage allowing for quicker regulation in response to extracellular hormones or changes in the environment. Please note that even though the regulation of NHE3 activity by LPA and elevated Ca^{2+} is accompanied by an increase in the NHE3 mobile fraction and dissociation of NHE3 from NHERF2 (17, 21), it does not involve global changes in the plasma membrane mobility of the NHERF proteins.

NHERF2 but not NHERF1 was required for the stimulation of NHE3 by LPA (10) and inhibition by the calcium ionophore A23187 (21). The specificity of NHERF proteins involved in NHE3 regulation by different pathways has been mainly attributed to their PDZ domains. Multiple studies have shown that the NHERF2 N-terminal PDZ domains but not those of NHERF1 play important roles in NHE3 regulation by binding to specific PDZ ligands such as SGK1, PLCβ3, and LPA_5 receptors (10, 11, 16). Previously, NHERF2Δ30 (lacking only the EBD) was studied and failed to support NHE3 inhibition by elevated $[Ca^{2+}]_i$ (21). Although this was interpreted as indicating that the EBD is required for NHERF2 regulation of NHE3 activity, in fact, NHERF2Δ30 was not localized to the microvilli. An advantage of this study is that chimeras NHERF2-1C, NHERF2-1E, and NHERF2-1–2 properly localized to the microvilli. These chimeras did not allow 4-Br-A23187 to inhibit the NHE3 activity and LPA/LPA_5 receptors to increase the NHE3 activity. Also, the NHE3 mobile fraction was not increased by LPA/LPA_5 receptors in the presence of NHERF2-1C as occurred with wild type NHERF2. Thus, the EBD of NHERF2 is not only required for NHE3 regulation but also cannot be replaced by the EBD of NHERF1. Moreover, the same is true for the nonconserved NHERF2 sequences between PDZ2 and the EBD. We conclude that the EBD and the upstream nonconserved sequences of NHERF2 following the PDZ2 domain are both required for the regulation of NHE3. We hypothesize that these two contiguous domains form a unique C-terminal domain functioning together for NHE3 regulation, although whether they physically interact or undergo direct cross-talk is unknown. Our studies show that NHERF2 is distinguished from NHERF1 not only by its specific PDZ domains but also by its unique C terminus, both of which must be considered in evaluating the specificity of their effects.

The role of this NHERF2 C-terminal domain in NHE3 regulation remains incompletely understood in detail, but it should be considered in light of the other characteristics of NHERF2 function that we showed were related to this domain. These include the slower BB mobility of NHERF2 compared with NHERF1 and NHERF3, its lesser detergent solubility, and the larger multiprotein complexes formed by NHERF2. In OK cells, NHERF2 has a smaller diffusion coefficient than NHERF1, consistent with studies in JEG-3 cells (32). It was previously established that the C-terminal EBDs of NHERF1 and NHERF2 contribute to their microvillus anchoring (21, 38, 40). The EBD of NHERF1 has higher affinity for ERM proteins than does the EBD of NHERF2 (39), leading to the suggestion that NHERF1 should be anchored more stably and move more slowly unless there are additional mechanisms anchoring NHERF2 into the microvillus. Indeed, the nonconserved region between PDZ2

and EBD of NHERF2 represents such an additional anchoring mechanism. Another difference between NHERF1 and NHERF2 relates to their different locations in the renal microvillus, with NHERF2 localized more in the microvillus base, although NHERF1 is more uniformly distributed along the microvillus (14). Whether the NHERF2 C terminus also determines its localization at the microvillar base is not known.

Some understanding of the regulatory contributions of the NHERF2 C-terminal tail after PDZ2 was already known from previous studies. This part of NHERF2 is required for interaction with both NHE3 (23) and α-actinin-4 (53). However, the specific NHERF2 C-terminal sequences involved had not been characterized. Chimera NHERF2-1C and wild type NHERF2 associate with NHE3 similarly strongly, suggesting that the nonconserved C-terminal region is not required for interaction with NHE3 and rather it is the sequences just downstream of PDZ2 that are involved. α-Actinin-4 has been shown to be necessary for elevated Ca^{2+} inhibition of NHE3 (53). By co-immunoprecipitation, chimera NHERF2-1C and NHERF1-2C both associate with α-actinin-4 much more weakly compared with wild type NHERF2.[4] This is consistent with previous results that interaction between NHERF2 and α-actinin-4 requires both the PDZ2 domain of NHERF2 and the C terminus after PDZ2 and probably contributes to the explanation for why NHERF2-1C does not support elevated Ca^{2+} inhibition of NHE3. The complex size analysis by sucrose gradient ultracentrifugation suggests that NHERF2 C-terminal domain is directly involved in scaffolding other molecules into large multiprotein complexes. But the proteins that bind to this NHERF2 domain to produce the reduced NHERF2 mobility compared with NHERF1 have not been identified. Important roles of NHERF2 have been implicated in NHE3 regulation by cGMP, elevated Ca^{2+}, D-glucose, and LPA (8, 10, 20, 54). Further identification of additional NHERF2 C-terminal binding partners and their involvement in NHE3 regulation should help clarify the roles of NHERF2 in regulation of NHE3 and of its many other ligands.

Membrane/cytoskeleton-associated NHERF1 and NHERF2 both exist in detergent-insoluble fractions, which include not only lipid rafts but also cytoskeleton-associated complexes. How much lipid raft association contributes to the detergent insolubility of NHERF1 and NHERF2 is unknown, but we believe lipid rafts play a minor role in OK cells because the lipid raft components of NHERF1 and NHERF2 are not significantly different by our methods. It is more likely that the cytoskeleton-associated complexes formed by NHERF1 and NHERF2 account for their different detergent-insoluble distributions. In complex size analysis by sucrose gradient ultracentrifugation, the results represent a transient state of a dynamic dissociation process due to gradient separation. The larger size of NHERF2 complexes determined by this method suggests that NHERF2 associates with the cytoskeleton complex more tightly. This could further explain its higher resistance to detergent solubilization as well as its slower mobility rate.

Along with the progress of our work in polarized renal epithelial cells, two reports were recently published showing similarly that NHERF1 and NHERF2 are mostly mobile in rat osteosarcoma 17/2.8 ROS cells (31) and human placental choriocarcinoma JEG-3 cells (32). These studies mainly focused on the study of NHERF1 mobility, and both studied the dependence of NHERF1 mobility on PDZ interactions (31, 32). Their results, however, seem to be contradictory. In ROS cells, overexpression of the PDZ ligand parathyroid hormone receptor reduced the mobility rate of NHERF1. In JEG-3 cells, overexpression of the PDZ ligand EPI64 increased the mobility rate of NHERF1, whereas mutation in the PDZ domains decreased the mobility rate. In contrast, in our studies with OK cells, neither overexpression of NHE3 nor mutations of the GYGF in the PDZ domains significantly affected the NHERF1 or NHERF2 mobility rates. Given that all three studies were performed with different cell types and different ligands, and even the mutations used to disrupt PDZ domains were slightly different (32, 55), it is not possible to further account for the different results currently.

In summary, NHERF1, NHERF2, and NHERF3 were highly mobile in the microvillus, suggesting they are anchoring their transmembrane ligands in a dynamic equilibrium. By comparison of mobility rates of NHERF2 and NHERF1, an additional functionally important C-terminal domain of NHERF2 was identified that determines its slower mobility and is involved in the formation of large multiprotein complexes and in the regulation of NHE3 activity and mobility. This C-terminal domain should be considered in future attempts to understand how NHERF2 takes part in the regulation of NHE3 and its many plasma membrane binding partners.

Acknowledgments—We thank John Gibas and Molee Chakraborty (Johns Hopkins University) for technical assistance. We thank Dr. Chris Yun (Emory University) for providing rabbit polyclonal antibody against NHERF2 and plasmid pcDNA3.1-LPA5R. We thank Dr. Jerrold Turner (University of Chicago) for providing the Caco-2/bbe cell line. We acknowledge use of the Kudsi Imaging Core Facility of the Conte Hopkins Digestive Disease Basic and Translational Research Core Center (supported by National Institutes of Health Grant P30DK089502).

[4] J. Yang and M. Donowitz, unpublished data.

REFERENCES

1. Lange, K. (2011) Fundamental role of microvilli in the main functions of differentiated cells: Outline of an universal regulating and signaling system at the cell periphery. *J. Cell. Physiol.* **226,** 896–927
2. Brant, S. R., Yun, C. H., Donowitz, M., and Tse, C. M. (1995) Cloning, tissue distribution, and functional analysis of the human Na^+/N^+ exchanger isoform, NHE3. *Am. J. Physiol.* **269,** C198–C206
3. Schultheis, P. J., Clarke, L. L., Meneton, P., Miller, M. L., Soleimani, M., Gawenis, L. R., Riddle, T. M., Duffy, J. J., Doetschman, T., Wang, T., Giebisch, G., Aronson, P. S., Lorenz, J. N., and Shull, G. E. (1998) Renal and intestinal absorptive defects in mice lacking the NHE3 Na^+/H^+ exchanger. *Nat. Genet.* **19,** 282–285
4. Donowitz, M., and Li, X. (2007) Regulatory binding partners and complexes of NHE3. *Physiol. Rev.* **87,** 825–872
5. Ardura, J. A., and Friedman, P. A. (2011) Regulation of G protein-coupled receptor function by Na^+/H^+ exchange regulatory factors. *Pharmacol. Rev.* **63,** 882–900
6. Romero, G., von Zastrow, M., and Friedman, P. A. (2011) Role of PDZ proteins in regulating trafficking, signaling, and function of GPCRs: means, motif, and opportunity. *Adv. Pharmacol.* **62,** 279–314

7. Weinman, E. J., Steplock, D., Wang, Y., and Shenolikar, S. (1995) Characterization of a protein cofactor that mediates protein kinase A regulation of the renal brush border membrane Na^+-H^+ exchanger. *J. Clin. Invest.* **95,** 2143–2149
8. Sarker, R., Valkhoff, V. E., Zachos, N. C., Lin, R., Cha, B., Chen, T. E., Guggino, S., Zizak, M., de Jonge, H., Hogema, B., and Donowitz, M. (2011) NHERF1 and NHERF2 are necessary for multiple but usually separate aspects of basal and acute regulation of NHE3 activity. *Am. J. Physiol. Cell Physiol.* **300,** C771–C782
9. Murtazina, R., Kovbasnjuk, O., Chen, T. E., Zachos, N. C., Chen, Y., Kocinsky, H. S., Hogema, B. M., Seidler, U., de Jonge, H. R., and Donowitz, M. (2011) NHERF2 is necessary for basal activity, second messenger inhibition, and LPA stimulation of NHE3 in mouse distal ileum. *Am. J. Physiol. Cell Physiol.* **301,** C126–C136
10. Lin, S., Yeruva, S., He, P., Singh, A. K., Zhang, H., Chen, M., Lamprecht, G., de Jonge, H. R., Tse, M., Donowitz, M., Hogema, B. M., Chun, J., Seidler, U., and Yun, C. C. (2010) Lysophosphatidic acid stimulates the intestinal brush border Na^+/H^+ exchanger 3 and fluid absorption via LPA(5) and NHERF2. *Gastroenterology* **138,** 649–658
11. Yun, C. C., Chen, Y., and Lang, F. (2002) Glucocorticoid activation of Na^+/H^+ exchanger isoform 3 revisited. The roles of SGK1 and NHERF2. *J. Biol. Chem.* **277,** 7676–7683
12. Cinar, A., Chen, M., Riederer, B., Bachmann, O., Wiemann, M., Manns, M., Kocher, O., and Seidler, U. (2007) NHE3 inhibition by cAMP and Ca^{2+} is abolished in PDZ-domain protein PDZK1-deficient murine enterocytes. *J. Physiol.* **581,** 1235–1246
13. Zachos, N. C., Hodson, C., Kovbasnjuk, O., Li, X., Thelin, W. R., Cha, B., Milgram, S., and Donowitz, M. (2008) Elevated intracellular calcium stimulates NHE3 activity by an IKEPP (NHERF4)-dependent mechanism. *Cell. Physiol. Biochem.* **22,** 693–704
14. Wade, J. B., Liu, J., Coleman, R. A., Cunningham, R., Steplock, D. A., Lee-Kwon, W., Pallone, T. L., Shenolikar, S., and Weinman, E. J. (2003) Localization and interaction of NHERF isoforms in the renal proximal tubule of the mouse. *Am. J. Physiol. Cell Physiol.* **285,** C1494–C1503
15. Cotton, L. M., Rodriguez, C. M., Suzuki, K., Orgebin-Crist, M. C., and Hinton, B. T. (2010) Organic cation/carnitine transporter, OCTN2, transcriptional activity is regulated by osmotic stress in epididymal cells. *Mol. Reprod. Dev.* **77,** 114–125
16. Donowitz, M., Cha, B., Zachos, N. C., Brett, C. L., Sharma, A., Tse, C. M., and Li, X. (2005) NHERF family and NHE3 regulation. *J. Physiol.* **567,** 3–11
17. Cha, B., Zhu, X. C., Chen, W., Jones, M., Ryoo, S., Zachos, N. C., Chen, T. E., Lin, R., Sarker, R., Kenworthy, A. K., Tse, M., Kovbasnjuk, O., and Donowitz, M. (2010) NHE3 mobility in brush borders increases upon NHERF2-dependent stimulation by lysophosphatidic acid. *J. Cell Sci.* **123,** 2434–2443
18. Brown, J. W., and McKnight, C. J. (2010) Molecular model of the microvillar cytoskeleton and organization of the brush border. *PLoS One* **5,** e9406
19. Cha, B., Kenworthy, A., Murtazina, R., and Donowitz, M. (2004) The lateral mobility of NHE3 on the apical membrane of renal epithelial OK cells is limited by the PDZ domain proteins NHERF1/2, but is dependent on an intact actin cytoskeleton as determined by FRAP. *J. Cell Sci.* **117,** 3353–3365
20. Lin, R., Murtazina, R., Cha, B., Chakraborty, M., Sarker, R., Chen, T. E., Lin, Z., Hogema, B. M., de Jonge, H. R., Seidler, U., Turner, J. R., Li, X., Kovbasnjuk, O., and Donowitz, M. (2011) D-Glucose acts via sodium/glucose cotransporter 1 to increase NHE3 in mouse jejunal brush border by a Na^+/H^+ exchange regulatory factor 2-dependent process. *Gastroenterology* **140,** 560–571
21. Zhu, X., Cha, B., Zachos, N. C., Sarker, R., Chakraborty, M., Chen, T. E., Kovbasnjuk, O., and Donowitz, M. (2011) Elevated calcium acutely regulates dynamic interactions of NHERF2 and NHE3 in OK cell microvilli. *J. Biol. Chem.* **286,** 34486–34496
22. Seidler, U., Singh, A. K., Cinar, A., Chen, M., Hillesheim, J., Hogema, B., and Riederer, B. (2009) The role of the NHERF family of PDZ scaffolding proteins in the regulation of salt and water transport. *Ann. N.Y. Acad. Sci.* **1165,** 249–260
23. Yun, C. H., Lamprecht, G., Forster, D. V., and Sidor, A. (1998) NHE3 kinase A regulatory protein E3KARP binds the epithelial brush border Na^+/H^+ exchanger NHE3 and the cytoskeletal protein ezrin. *J. Biol. Chem.* **273,** 25856–25863
24. Murtazina, R., Kovbasnjuk, O., Donowitz, M., and Li, X. (2006) Na^+/H^+ exchanger NHE3 activity and trafficking are lipid Raft-dependent. *J. Biol. Chem.* **281,** 17845–17855
25. McKinney, S. A., Murphy, C. S., Hazelwood, K. L., Davidson, M. W., and Looger, L. L. (2009) A bright and photostable photoconvertible fluorescent protein. *Nat. Methods* **6,** 131–133
26. Ellenberg, J., Siggia, E. D., Moreira, J. E., Smith, C. L., Presley, J. F., Worman, H. J., and Lippincott-Schwartz, J. (1997) Nuclear membrane dynamics and reassembly in living cells: targeting of an inner nuclear membrane protein in interphase and mitosis. *J. Cell Biol.* **138,** 1193–1206
27. Mavrakis, M., Rikhy, R., Lilly, M., and Lippincott-Schwartz, J. (2008) Fluorescence imaging techniques for studying *Drosophila* embryo development. *Curr. Protoc. Cell Biol.* Chapter 4, Unit 4.18
28. Li, X., Galli, T., Leu, S., Wade, J. B., Weinman, E. J., Leung, G., Cheong, A., Louvard, D., and Donowitz, M. (2001) Na^+-H^+ exchanger 3 (NHE3) is present in lipid rafts in the rabbit ileal brush border: a role for rafts in trafficking and rapid stimulation of NHE3. *J. Physiol.* **537,** 537–552
29. Li, X., Zhang, H., Cheong, A., Leu, S., Chen, Y., Elowsky, C. G., and Donowitz, M. (2004) Carbachol regulation of rabbit ileal brush border Na^+-H^+ exchanger 3 (NHE3) occurs through changes in NHE3 trafficking and complex formation and is Src-dependent. *J. Physiol.* **556,** 791–804
30. Haggie, P. M., Stanton, B. A., and Verkman, A. S. (2004) Increased diffusional mobility of CFTR at the plasma membrane after deletion of its C-terminal PDZ-binding motif. *J. Biol. Chem.* **279,** 5494–5500
31. Ardura, J. A., Wang, B., Watkins, S. C., Vilardaga, J. P., and Friedman, P. A. (2011) Dynamic Na^+-H^+ exchanger regulatory factor-1 association and dissociation regulate parathyroid hormone receptor trafficking at membrane microdomains. *J. Biol. Chem.* **286,** 35020–35029
32. Garbett, D., and Bretscher, A. (2012) PDZ interactions regulate rapid turnover of the scaffolding protein EBP50 in microvilli. *J. Cell Biol.* **198,** 195–203
33. Cole, J. A., Forte, L. R., Krause, W. J., and Thorne, P. K. (1989) Clonal sublines that are morphologically and functionally distinct from parental OK cells. *Am. J. Physiol.* **256,** F672–F679
34. Padányi, R., Xiong, Y., Antalffy, G., Lór, K., Pászty, K., Strehler, E. E., and Enyedi, A. (2010) Apical scaffolding protein NHERF2 modulates the localization of alternatively spliced plasma membrane Ca^{2+} pump 2B variants in polarized epithelial cells. *J. Biol. Chem.* **285,** 31704–31712
35. Lee, H. J., and Zheng, J. J. (2010) PDZ domains and their binding partners: structure, specificity, and modification. *Cell Commun. Signal.* **8,** 8
36. Karthikeyan, S., Leung, T., and Ladias, J. A. (2002) Structural determinants of the Na^+/H^+ exchanger regulatory factor interaction with the β2 adrenergic and platelet-derived growth factor receptors. *J. Biol. Chem.* **277,** 18973–18978
37. Weinman, E. J., Wang, Y., Wang, F., Greer, C., Steplock, D., and Shenolikar, S. (2003) A C-terminal PDZ motif in NHE3 binds NHERF-1 and enhances cAMP inhibition of sodium-hydrogen exchange. *Biochemistry* **42,** 12662–12668
38. Finnerty, C. M., Chambers, D., Ingraffea, J., Faber, H. R., Karplus, P. A., and Bretscher, A. (2004) The EBP50-moesin interaction involves a binding site regulated by direct masking on the FERM domain. *J. Cell Sci.* **117,** 1547–1552
39. Terawaki, S., Maesaki, R., and Hakoshima, T. (2006) Structural basis for NHERF recognition by ERM proteins. *Structure* **14,** 777–789
40. Morales, F. C., Takahashi, Y., Momin, S., Adams, H., Chen, X., and Georgescu, M. M. (2007) NHERF1/EBP50 head-to-tail intramolecular interaction masks association with PDZ domain ligands. *Mol. Cell. Biol.* **27,** 2527–2537
41. Weinman, E. J., Steplock, D., Wade, J. B., and Shenolikar, S. (2001) Ezrin binding domain-deficient NHERF attenuates cAMP-mediated inhibition of Na^+/H^+ exchange in OK cells. *Am. J. Physiol. Renal Physiol.* **281,** F374–F380
42. Itoh, K., Sakakibara, M., Yamasaki, S., Takeuchi, A., Arase, H., Miyazaki, M., Nakajima, N., Okada, M., and Saito, T. (2002) Cutting edge: negative regulation of immune synapse formation by anchoring lipid raft to cyto-

skeleton through Cbp-EBP50-ERM assembly. *J. Immunol.* **168,** 541–544
43. Lissner, S., Nold, L., Hsieh, C. J., Turner, J. R., Gregor, M., Graeve, L., and Lamprecht, G. (2010) Activity and PI3-kinase-dependent trafficking of the intestinal anion exchanger down-regulated in adenoma depend on its PDZ interaction and on lipid rafts. *Am. J. Physiol. Gastrointest. Liver Physiol.* **299,** G907–G920
44. Berryman, M., Gary, R., and Bretscher, A. (1995) Ezrin oligomers are major cytoskeletal components of placental microvilli: a proposal for their involvement in cortical morphogenesis. *J. Cell Biol.* **131,** 1231–1242
45. Lee-Kwon, W., Kawano, K., Choi, J. W., Kim, J. H., and Donowitz, M. (2003) Lysophosphatidic acid stimulates brush border Na^+/H^+ exchanger 3 (NHE3) activity by increasing its exocytosis by an NHE3 kinase A regulatory protein-dependent mechanism. *J. Biol. Chem.* **278,** 16494–16501
46. Lee-Kwon, W., Kim, J. H., Choi, J. W., Kawano, K., Cha, B., Dartt, D. A., Zoukhri, D., and Donowitz, M. (2003) Ca^{2+}-dependent inhibition of NHE3 requires PKCα, which binds to E3KARP to decrease surface NHE3 containing plasma membrane complexes. *Am. J. Physiol. Cell Physiol.* **285,** C1527–C1536
47. Coscoy, S., Waharte, F., Gautreau, A., Martin, M., Louvard, D., Mangeat, P., Arpin, M., and Amblard, F. (2002) Molecular analysis of microscopic ezrin dynamics by two-photon FRAP. *Proc. Natl. Acad. Sci. U.S.A.* **99,** 12813–12818
48. Waharte, F., Brown, C. M., Coscoy, S., Coudrier, E., and Amblard, F. (2005) A two-photon FRAP analysis of the cytoskeleton dynamics in the microvilli of intestinal cells. *Biophys. J.* **88,** 1467–1478
49. Tyska, M. J., and Mooseker, M. S. (2002) MYO1A (brush border myosin I) dynamics in the brush border of LLC-PK1-CL4 cells. *Biophys. J.* **82,** 1869–1883
50. Weinman, E. J., Steplock, D., Cha, B., Kovbasnjuk, O., Frost, N. A., Cunningham, R., Shenolikar, S., Blanpied, T. A., and Donowitz, M. (2009) PTH transiently increases the percent mobile fraction of Npt2a in OK cells as determined by FRAP. *Am. J. Physiol. Renal Physiol.* **297,** F1560–F1565
51. Cha, B., Tse, M., Yun, C., Kovbasnjuk, O., Mohan, S., Hubbard, A., Arpin, M., and Donowitz, M. (2006) The NHE3 juxtamembrane cytoplasmic domain directly binds ezrin: dual role in NHE3 trafficking and mobility in the brush border. *Mol. Biol. Cell* **17,** 2661–2673
52. Han, W., Kim, K. H., Jo, M. J., Lee, J. H., Yang, J., Doctor, R. B., Moe, O. W., Lee, J., Kim, E., and Lee, M. G. (2006) Shank2 associates with and regulates Na^+/H^+ exchanger 3. *J. Biol. Chem.* **281,** 1461–1469
53. Kim, J. H., Lee-Kwon, W., Park, J. B., Ryu, S. H., Yun, C. H., and Donowitz, M. (2002) Ca^{2+}-dependent inhibition of Na^+/H^+ exchanger 3 (NHE3) requires an NHE3-E3KARP-α-actinin-4 complex for oligomerization and endocytosis. *J. Biol. Chem.* **277,** 23714–23724
54. Chen, M., Sultan, A., Cinar, A., Yeruva, S., Riederer, B., Singh, A. K., Li, J., Bonhagen, J., Chen, G., Yun, C., Donowitz, M., Hogema, B., de Jonge, H., and Seidler, U. (2010) Loss of PDZ-adaptor protein NHERF2 affects membrane localization and cGMP- and $[Ca^{2+}]$- but not cAMP-dependent regulation of Na^+/H^+ exchanger 3 in murine intestine. *J. Physiol.* **588,** 5049–5063
55. LaLonde, D. P., Garbett, D., and Bretscher, A. (2010) A regulated complex of the scaffolding proteins PDZK1 and EBP50 with ezrin contribute to microvillar organization. *Mol. Biol. Cell* **21,** 1519–1529